(RESEARCH ARTICLE)

Check for updates

Concentration of heavy minerals in Padma-river bar sediments from Bheramara to Ruppur using multispectral satellite data and petrographic analysis

Iftekharul Islam [1, *], Chayon Kumar Mondal [1], Md. Al Zabir Hassan Mithen [2], Md. Safayet Mostofa Sadit [1], Fatema Akter Mitu [1] and Mallika Das [1]

[1] Department of Geology and Mining, University of Rajshahi, Rajshahi 6205, Bangladesh.
[2] Department of Economics, University of Rajshahi, Rajshahi 6205, Bangladesh.

Abstract

This study investigates the heavy minerals of bar sediments in the Padma river, revealing high concentrations of economically significant minerals. Utilizing multispectral satellite data from Landsat-9 (OLI/TIRS) and processing through ENVI 5.3 and ArcGIS 10.8.2, we produced detailed zonation maps that highlight the distribution and concentration of various heavy minerals. Through the analysis, a range of valuable minerals has been identified including biotite, epidote, garnet, hornblende, kyanite, monazite, rutile, hematite, ilmenite, and magnetite, with garnet (13.99%), epidote (13.16%), hornblende (8.99%), kyanite (14.97%), and rutile (9.98%) being the most prevalent. Despite quartz not being classified as a heavy mineral, its high abundance adds to the economic value of the sediments. The study emphasizes the potential for eco-friendly and sustainable extraction methods to exploit these resources without causing significant environmental disruption. The findings suggest that the heavy minerals in the Padma River sediments, spanning from Bheramara to Ruppur, hold substantial economic promise for the region. This research underscores the importance of integrating remote sensing technology with traditional mineral analysis to optimize resource management and contribute to local economic development.

Keywords: Heavy minerals; Padma river; Multispectral; Petrographic

1. Introduction

Heavy minerals in Padma river bar sediments are highly enriched with economic mineral grade. Heavy minerals have a high specific gravity (SG > 2.8 g/cm³). Generally, heavy minerals are found in all sedimentary deposits. The most common heavy minerals in Padma river bar sediments are kyanite, garnet, epidote, hornblende, rutile, monazite, hematite, ilmenite, magnetite, etc. (Rahman et al., 2014; Rahman et al., 2016; Rahman et al., 2020) [1, 2, 3]. These heavy minerals are resistant to weathering and are stable compared to other lighter minerals. In the igneous and metamorphic rocks, the concentration of heavy minerals are very low, but the concentration is high in the placer deposits in the coastal shoreline, and the river beds because of the resistance to the chemical and physical weathering and having comparatively high density.

All types of minerals like heavy and light are carried by river water, and heavy minerals are deposited along the channel bars. The lighter minerals are carried away to the water by the wave action repeatedly. The concentration of the heavy minerals is further enriched by the action of wind on the bars. River morphology, continental geomorphology and the neotectonics are the important factors for the deposition of heavy mineral along with the bar sediments.

Last decades, cutting-edge space-borne satellite sensors have been widely and constantly used for geological mapping and mineral exploration (e.g., Chandrasekar et al., 2011; Ahmadirouhani et al., 2018; Rajendran & Nasir 2019; Bolouki

---

* Corresponding author: Iftekharul Islam

et al., 2019) [4, 5, 6, 7]. In recent times, remotely sensed data are also being used efficiently in different fields of geology, especially lithological mapping, mineral identifications, and hydrothermal alteration zone identifications on small or large scales (Reeves, 1975; Siegal & Gillespie, 1980; Carper, 1990; Gabr et al., 2010; Bedini, 2011; Tangestani et al., 2011; Van der Meer et al., 2012; Zoheir & Emam, 2014) [8, 9, 10, 11, 12, 13, 14, 15]. In this regard, multispectral satellite sensors, such as Landsat thematic mapper (TM), Landsat Enhanced thematic mapper (ETM+), and Landsat Operational Land Imager (OLI) having 7, 8 and 9 spectral bands respectively have been used for those processes (Qari et al., 2008; Sadeghi et al., 2015; Pournamdari et al., 2014; Adiri et al., 2016; Ourhzif et al., 2019) [16, 17, 18, 19, 20]. Imaging spectrometry, the systematic measurement of spectra and images in some bands, is a recognized technology for detecting and mapping minerals based on their reflectance signatures (Kruse et al., 2012) [21]. Chandrasekar et al. (2011) [4] described the value of using space techniques to find and observe various coastal features over a large area in a short time.

The main goals of the research are the identification of heavy minerals and their concentration, to prepare a spatial distribution zoning map of heavy minerals by using multispectral satellite images, and to explore the eco-friendly distribution of the economic heavy minerals in the field of study.

2. Study area

The study area includes channel bars near Bheramara and Ruppur, located at the center-western part of Bangladesh (Figure 1) and the major river Padma flowing along the area. The heavy minerals are transported and accumulated mainly by the Padma river. Tectonically, the study area is situated in the south-western part of Bogura Slope near the Palaeo Continental Slope (Guha, 1978; Reimann & Hiller, 1993) [22, 23]. Physiographically, the study area lies in Ganges Floodplain (GSB, 1990) [24].
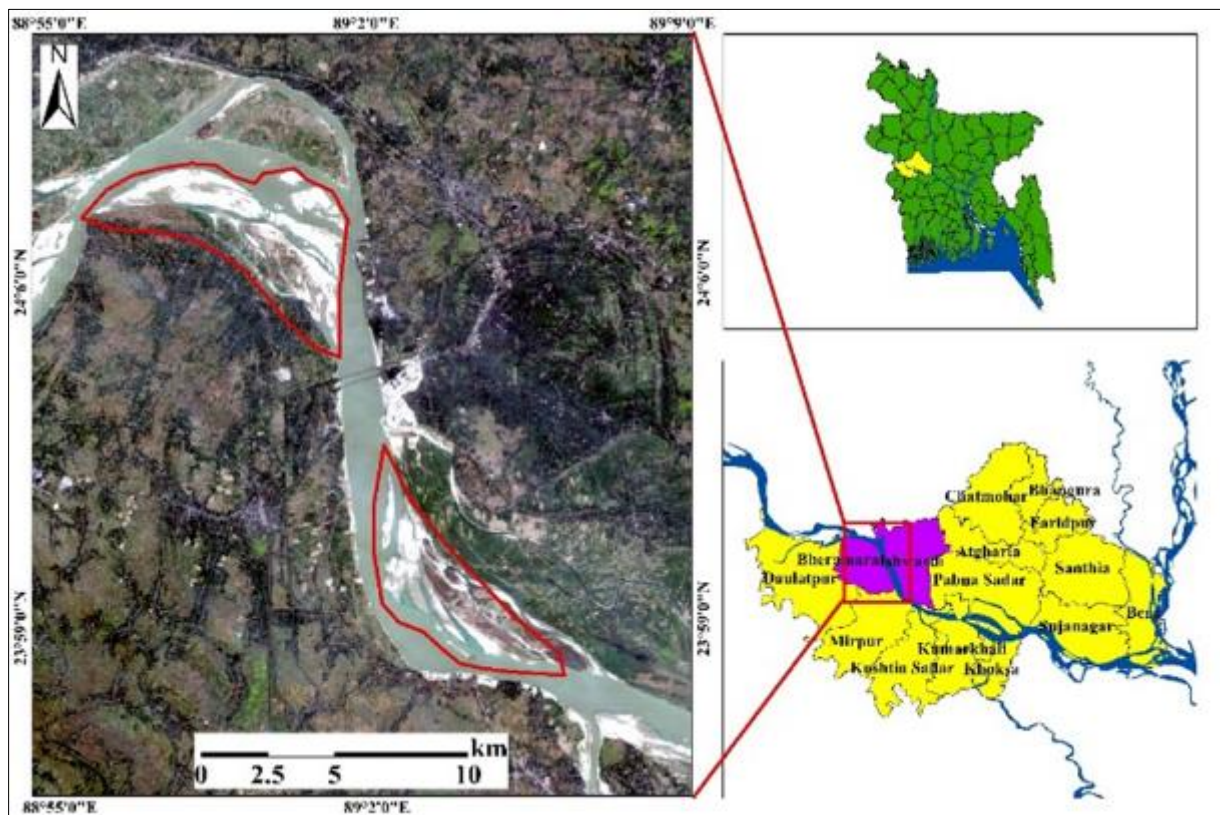

Figure 1 Location map of the study area

3. Materials and methods

The research work requires multispectral satellite data collection and processing, sample collection of bar sediments, sieve analysis, heavy mineral separation and microscopic observation. Different types of software have been used for

this research work including ENVI 5.3 and ArcGIS 10.8.2 to prepare zonation map of heavy mineral concentrations and their signatures.

3.1. Satellite data collection

Multispectral satellite data of the study area have been used for the digital image analysis. Landsat-9 OLI/TIRS image having 11 spectral bands have been used for this advanced spectral analysis process. The multispectral satellite data are collected from USGS Earth Explorer. Parameters of the Landsat-9 (OLI/TIRS) data are shown in Table 1 and spectral properties of the bands are shown in Table 2.

Table 1 Parameters of the Landsat-9 (OLI/TIRS) data (Source: USGS Earth Explorer)

Data set	Landsat-9
Sensor type	Operational Land Imager (OLI) / Thermal Infrared Sensor (TIRS)
Number of bands	11
Spatial Resolution	30 m (Except Band 8, 10, 11)
Product ID	LC09_L1TP_138043_20221216_20230317_02_T1
Path	138
Row	43
Date acquired	December 16, 2022
Scene center time	04:31:02.8696669Z
Scene size	185 km by 180 km
Altitude	705 km
Cloud cover	0.43
Datum	WGS84
UTM zone	45

Table 2 Spectral properties of Landsat-9 (OLI/TIRS) bands

Bands	Wavelengths (µm)	Resolution (m)
Band 1 : Coastal Aerosol	0.43 – 0.45	30
Band 2: Blue	0.45 – 0.51	30
Band 3: Green	0.53 – 0.59	30
Band 4: Red	0.64 – 0.67	30
Band 5: Near Infrared	0.85 – 0.88	30
Band 6: SWIR 1	1.57 – 1.65	30
Band 7: SWIR 2	2.11 – 2.29	30
Band 8: Panchromatic (PAN)	0.50 – 0.68	15
Band 9: Cirrus	1.36 – 1.38	30
Band 10: TIRS 1	10.60 – 11.19	100
Band 11: TIRS 2	11.50 – 12.51	100

3.2. Satellite data processing

Satellite data processing includes the continuous process of (i) atmospheric correction of Landsat-9 OLI/TIRS data by radiometric and reflectance calibration, (ii) applying minimum noise fraction transformation, (iii) implication of pixel purity index, (iv) N-dimensional visualization to extract endmember spectra, (v) identification of target heavy mineral from the comparison of endmember spectra and USGS spectral library spectra, and (vi) preparation of heavy mineral concentration zoning map using spectral angle mapper tool. The main point of this method is to reduce the dimension of the satellite image both in spatial and spectral perspectives to collect, locate and identify the few key spectra (endmembers) which are the desired mineral's signs (Kruse et al., 2003) [25]. Location of the different heavy minerals have been identified and the heavy mineral concentration zoning map of the study area have been prepared.

3.2.1. Atmospheric correction of satellite image

Atmospheric correction has been implemented to remove the atmospheric effects from the satellite data using atmospheric correction modeling tool. Atmospheric correction has been performed by using fast line of sight atmospheric analysis of spectral hypercubes (FLAASH) tool. After getting the required calibration parameters of the multispectral data, the model compensates for the atmospheric effects and recovers the spectral reflectance from the radiance (Chandrasekar et al., 2011) [4]. After the completion of the atmospheric correction, the data is ready for the other steps of satellite image processing.

3.2.2. Minimum noise fraction transformation

Minimum noise fraction (MNF) is the transformation process which is used to reduce noise in the data, to determine the natural dimensionality of data, to decrease computational necessities for further processing (Boardman and Kruse, 1994) [26]. It computes the information on noise statistics to essentially eliminate the noise from the dataset. In ENVI, the MNF transformation is used by performing a forward MNF transformation to remove noise from data. Eigenvalue plot for different MNF bands of OLI/TIRS data is shown in Figure 2. After the completion of the MNF process, the resulted curve revealed that the band no. 1 has the highest eigenvalues. MNF transformed band images of the study area are shown in Figure 3.
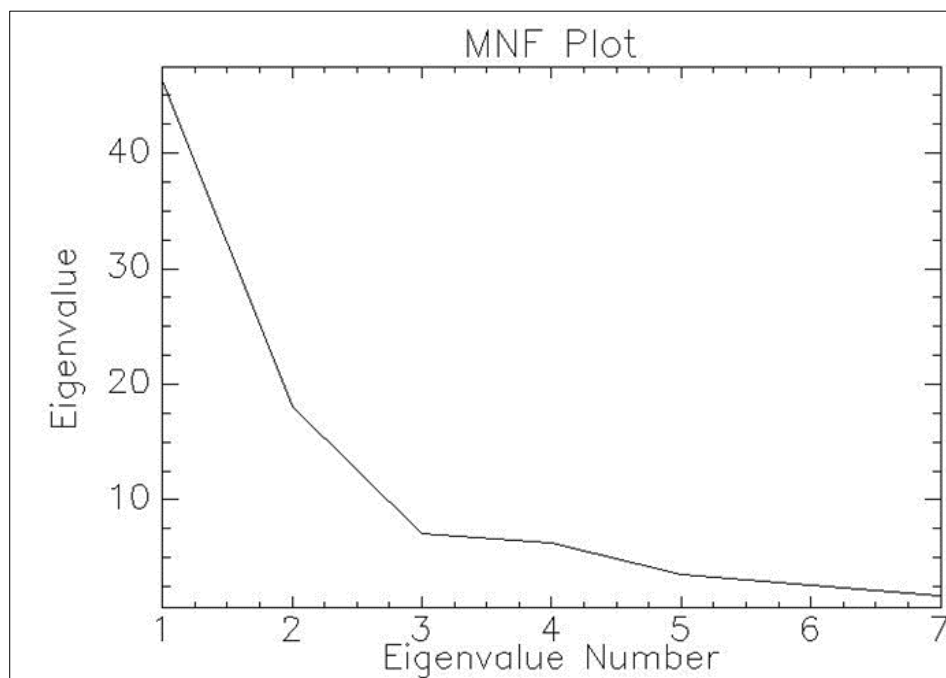

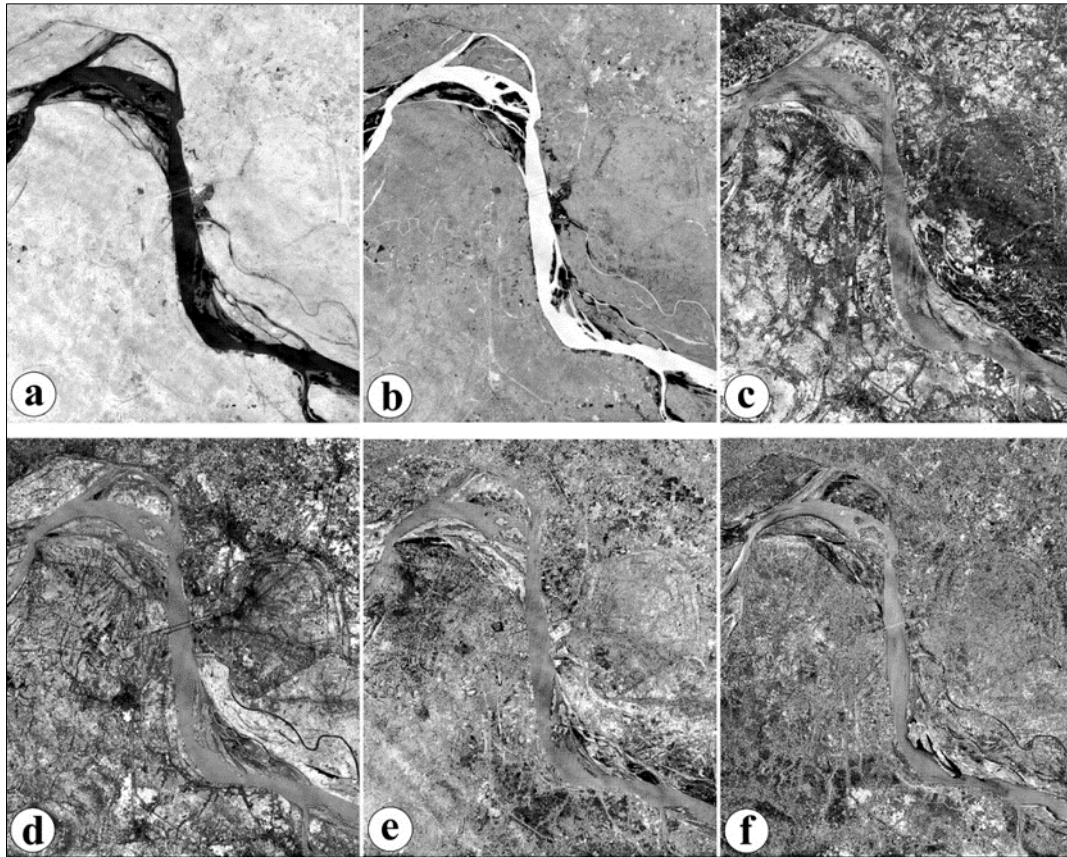**Figure 2** Eigenvalue plot for different MNF bands of OLI/TIRS data

Figure 3 Different MNF band images of the area: a. MNF band 1, b. MNF band 2, c. MNF band 3, d. MNF band 4, e. MNF band 5, f. MNF band 6
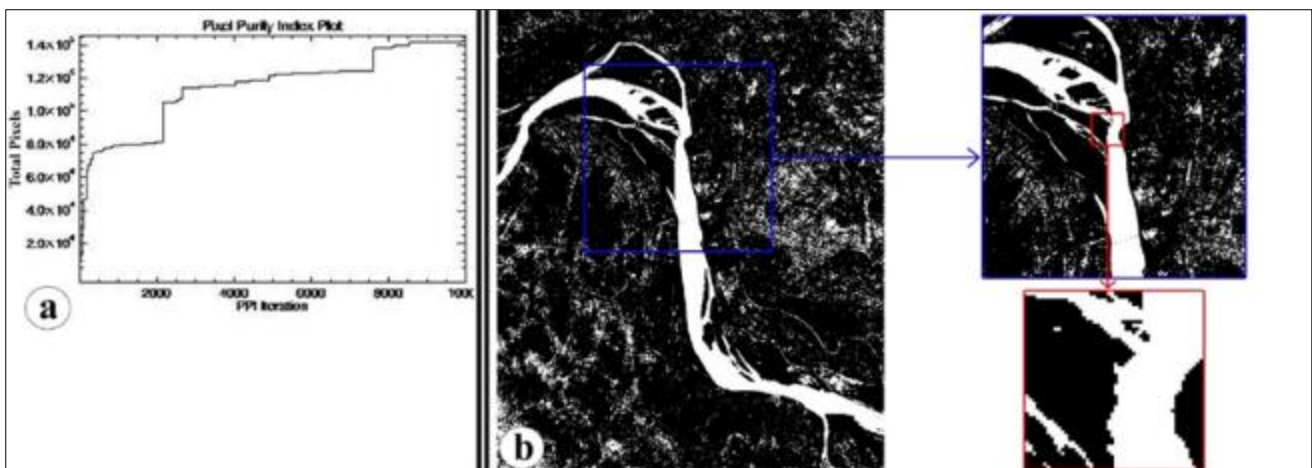
3.2.3. Pixel purity index

Figure 4 a. Pixel Purity Index plot between the PPI Iteration and Total Pixels, and b. Pixel Purity Index generated end-members image

Pixel purity index (PPI) is process to find the most pure pixel in the spectral data set (Boardman, 1993; Boardman et al., 1995) [27, 28]. It is one of the most commonly used endmember extraction algorithms for multispectral image analysis. The PPI reduces the number of pixels to be analyzed in a data set and leads us to attain the spectrally unique target minerals or endmembers. PPI plot generated from this process which showing relations between total number of extreme pixels and the PPI iterations (Figure 4). In the PPI parameters, the iterations represent the number of times that the data is projected onto the random vector. As a function of the number of iterations, this plot displays the total number of extreme pixels meeting the threshold criterion found by the PPI processing.

3.2.4. N-Dimensional visualization

N-dimensional visualizer is an integrated tool used to create pixel clouds using the MNF band in the n-dimensional space. In different directions and angles, the produced pixel clouds can be rotated and visualized (Figure 5). The visualizer allows to identify and separate the target endmembers present in the data from the main clusters (Chandrasekar et al., 2011) [4]. The selected endmembers are verified by matching and comparing their spectral signatures with the spectral reflectance from the USGS spectral library. By matching both the reflectance signatures, the names of the endmembers or minerals have been identified (Figure 6).
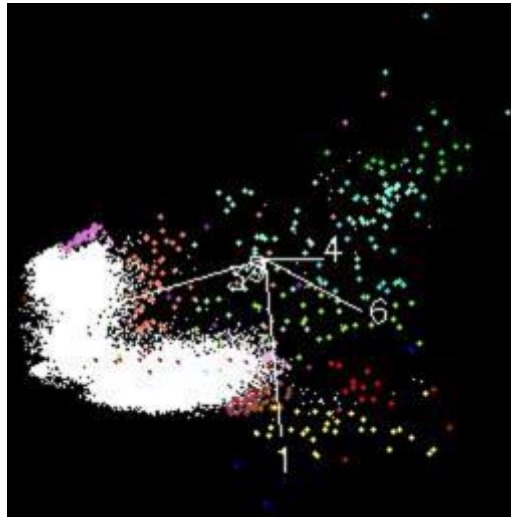

Figure 5 N-Dimensional Visualizer results showing the N-Dimension space of pixels
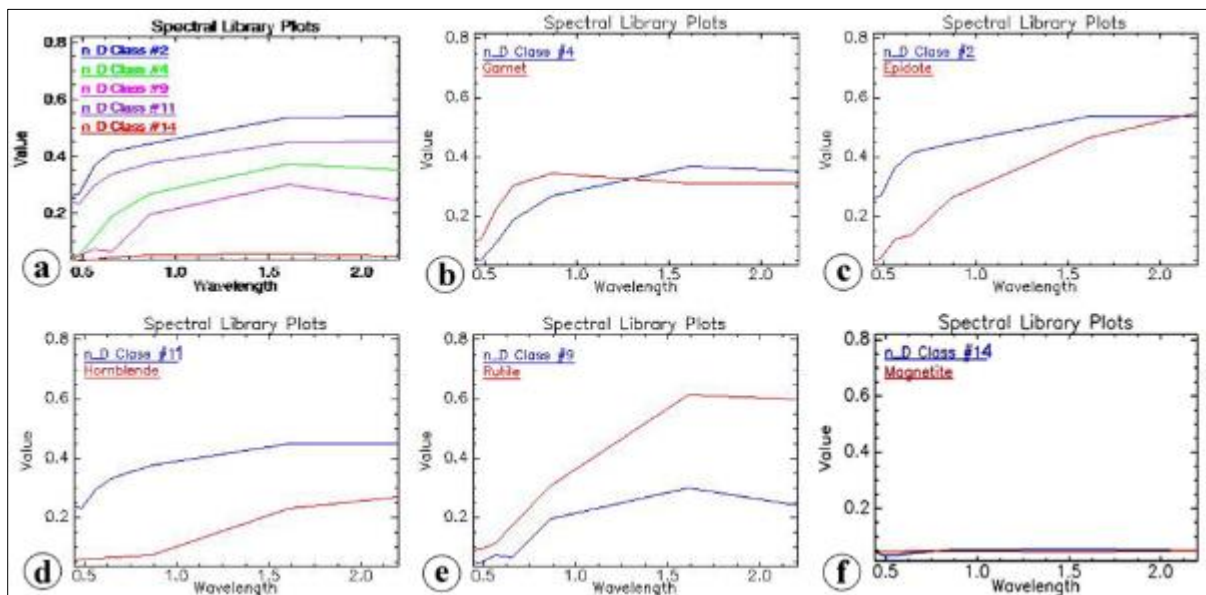

Figure 6 Spectral reflectance plots of the selected end-members almost closed to the normalized spectral plots of selected minerals obtained from the USGS spectral library

3.2.5. Spectral angle mapper

Spectral angle mapper (SAM) is an important method for the mapping of the mineral using the endmember spectral signatures. ENVI's spectral angle mapper maps the selected and confirmed target endmembers present in the data. Spectral angle between pixel spectrum and target spectrum is calculated by the SAM (Yuhas et al., 1992) [29]. SAM is the most used mapping tool for the mapping minerals by using hyperspectral or multispectral data. SAM is an automated

tool to compare image spectra, it calculates the similarity between two spectra, treating them as vectors in a space of dimensionality equal to the number of bands (Van der Meer and de Jong, 2003) [30]. Using SAM, the heavy mineral concentration zoning map of the area has been generated.

3.3. Sediment sample collection

Ten samples (five from channel bars of Padma near Bheramara and five near Ruppur) were collected from different spots of the study area to assess the accuracy of mineral assemblage classification. A hand operated sand auger was used to collect the samples. Locations of sediment samples are indicated in Figure 7.
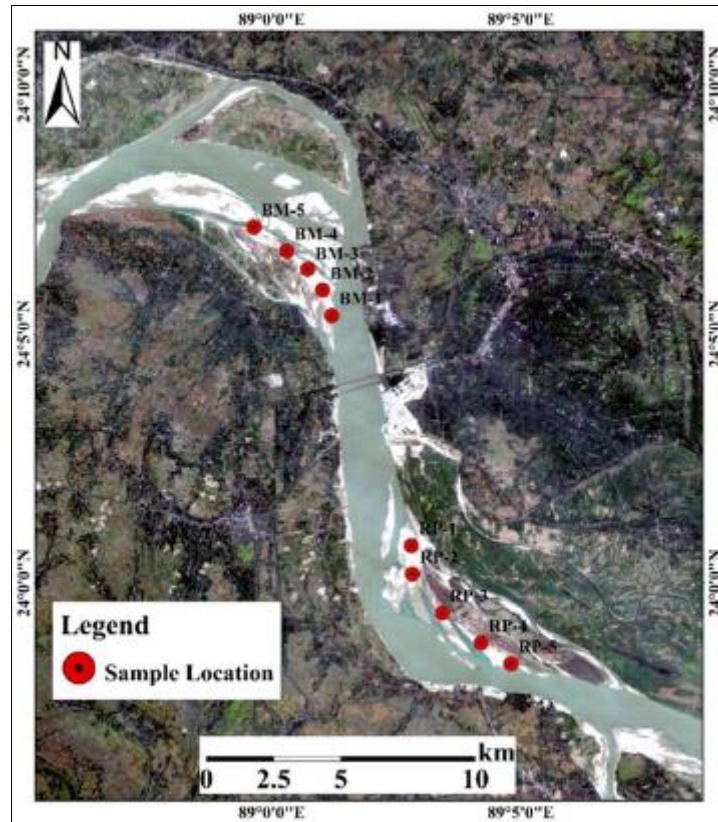

Figure 7 Location map of collected samples in the study area

3.4. Sieve analysis of sediments

One of the key descriptive characteristics of siliciclastic sedimentary rocks is their grain size, which is also one of its essential characteristics. The sizes of particles in a particular deposit reflect weathering and erosion processes, which generate particles of various sizes and the nature of subsequent transport processes (Boggs, 2009) [31]. It is a concern of the velocity and the mode of the transporting agent. The size of the particle is also a measure of a guide to the proximity of the source area. According to Friedman and Sanders (1978) [32], the velocity of the transporting medium generally helps to separate particles according to their size. Granule-silt-sized particles in unconsolidated sediments or sedimentary rocks that can be disaggregated are commonly measured using the sieving technique [31] with the help of the sieve shaker machine shown in Figure 8. After that, weight percentage of sediments from different mesh number has been measured to analyze the histograms (Figure 9), frequency curves (Figure 10) and cumulative curves (Figure 11) which help to describe the mode of transportation of the sediments all together with the minerals.

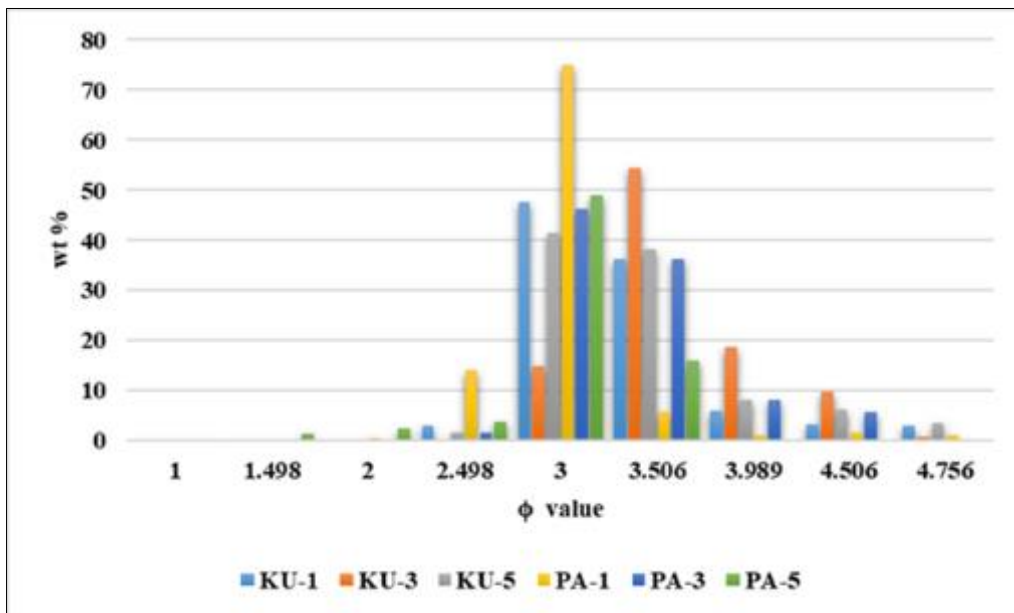**Figure 8** Grain size distribution using sieving method

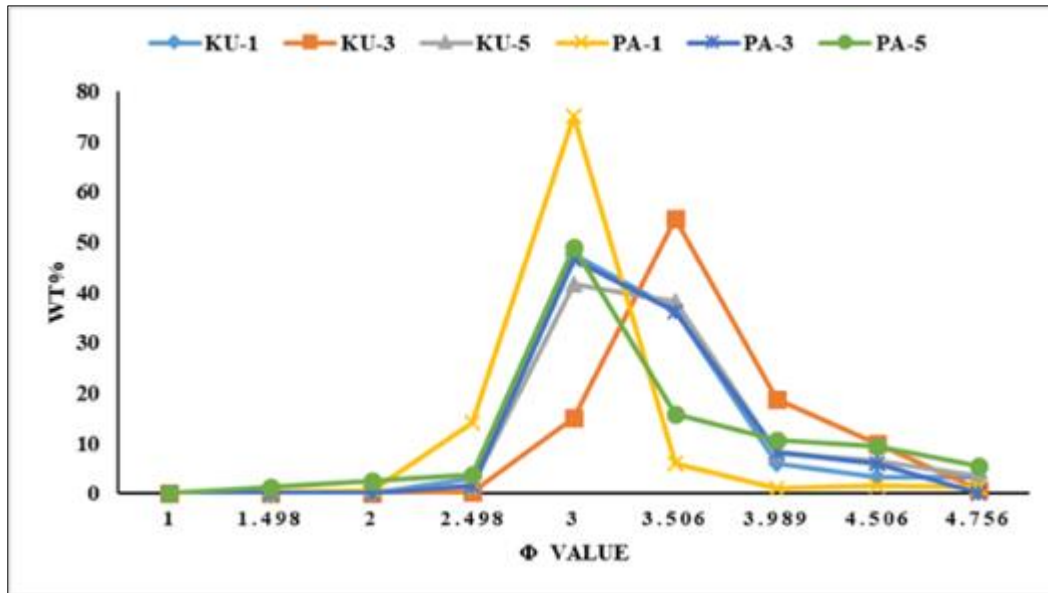**Figure 9** Histogram of different sediment samples in the study area

Figure 10 Frequency curves of different sediment samples in the study area
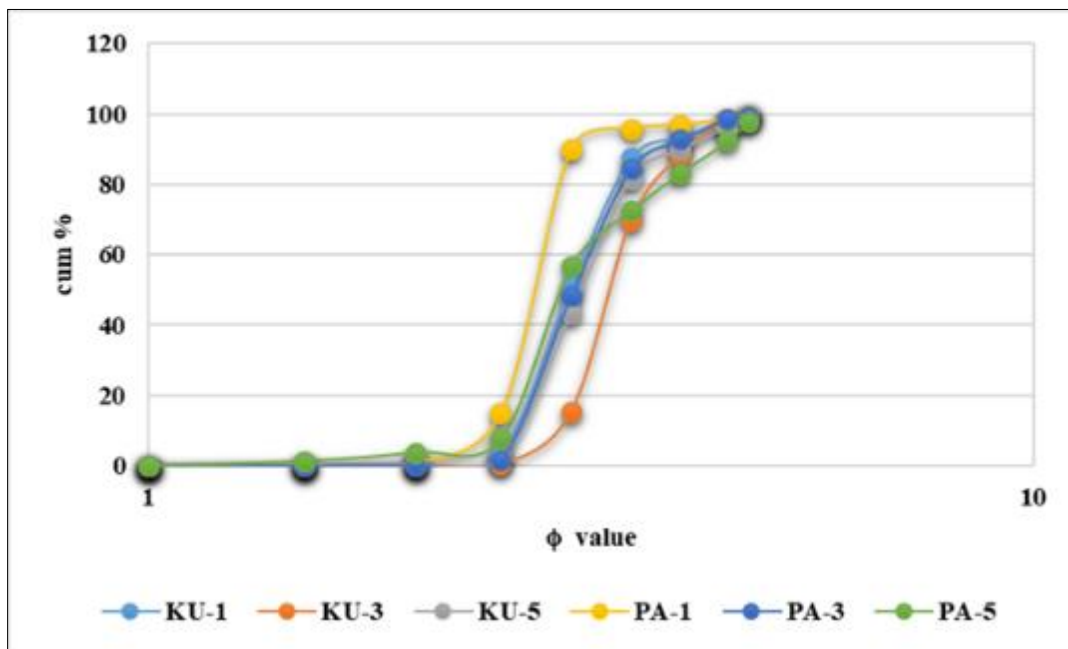

Figure 11 Cumulative curves of different sediment samples in the study area

3.5. Heavy mineral separation

The heavy mineral separation was carried out by the standard 1,1,2,2 tetrabromo ethane technique (specific gravity 2.96) using separating funnel fitted to iron rod stand with the help of clip (Figure 12). Using an iron ring filled with sand, filter paper was placed beneath the separating funnel in an open glass conical funnel. Taking considerable quantity of 1,1,2,2 tetrabromo ethane in the funnel, 100g of sample was poured in it. The heavy minerals were started to sink through the 1,1,2,2 tetrabromo ethane at the lower closed end of the clipped separating funnel. This position was kept for an hour together and with a regular interval of about half an hour, the samples were stirred. After setting the heavies, the grains of heavy minerals were separated by opening the lower end of separating funnel for a very short period with the help of clip. As soon as the heavy minerals were collected in the filter paper, the clip was closed. Then the funnel with 1,1,2,2 tetrabromo ethane was removed from the stand and the separated heavy minerals on the filter paper were

washed in the xylene, dried in the open air and preserved. The weight percentage of heavy and light minerals were measured again (Figure 13).

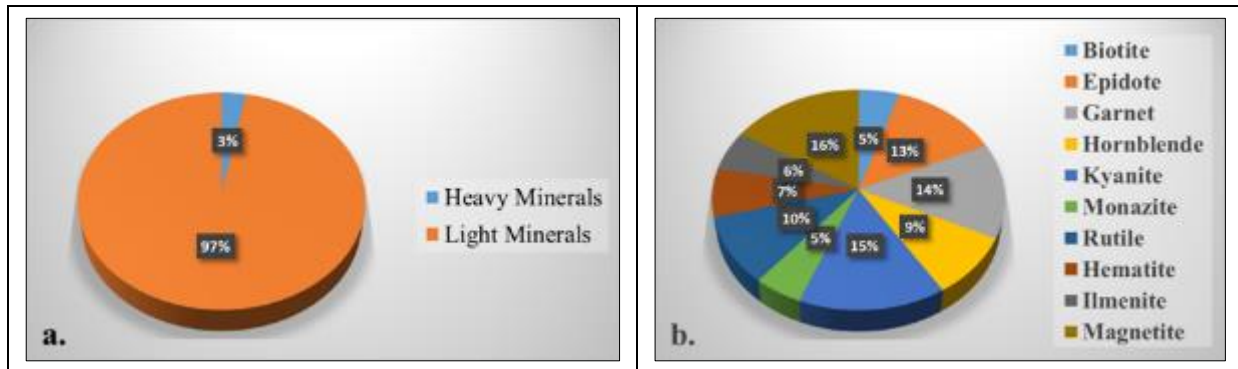**Figure 12** Heavy mineral separation using tetra-bromo ethane

Figure 13 π-chart showing the average a. weight percentage of light and heavy minerals, b. weight percentage of different heavy minerals in the study area

3.6. Microscopic observation

Taking considerable amount of liquid Canada Balsam on microscopic glass slide, it was heated by the heater. In this stage, the grains of heavy minerals put in the Canada Balsam, taking away the glass slides form the heater it was covered with cover slip of 25×25 mm. Maintaining this procedure in order to identify the individual heavy minerals, all 10 slides were examined under the petrographic microscope. The magnification (140x) was kept constant throughout the identification. For all the 10 slides of representative samples, total count of both opaque and non-opaque heavies were made for the computation of percentage frequency of various minerals (Figure 14).
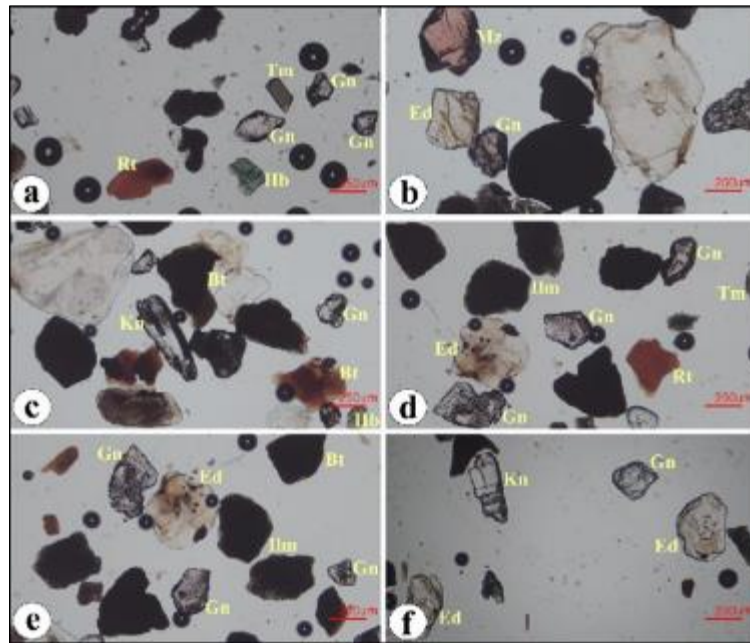
Figure 14 Microscopic view of the heavy minerals a., b. and c. near Bheramara, d., e. and f. near Ruppur.

4. Results and discussion

4.1. Heavy mineral zonation map from multispectral satellite data

From the satellite image analysis, using several bands and their iteration completion, the whole satellite image processes, and finally, considerable amounts of end members are being characterized. End members are obtained from heavy mineral spectra, however, this is clumsy in some places due to vegetation and water spectra in the area, causing some difficulty in identifying individual heavy mineral enrichment in an area from the spectral signatures. After comparing the USGS spectral library of minerals to the spectral charts of selected end members, it is confirmed that four types of heavy minerals are considered, garnet, epidote, hornblende and rutile (Figure 15).
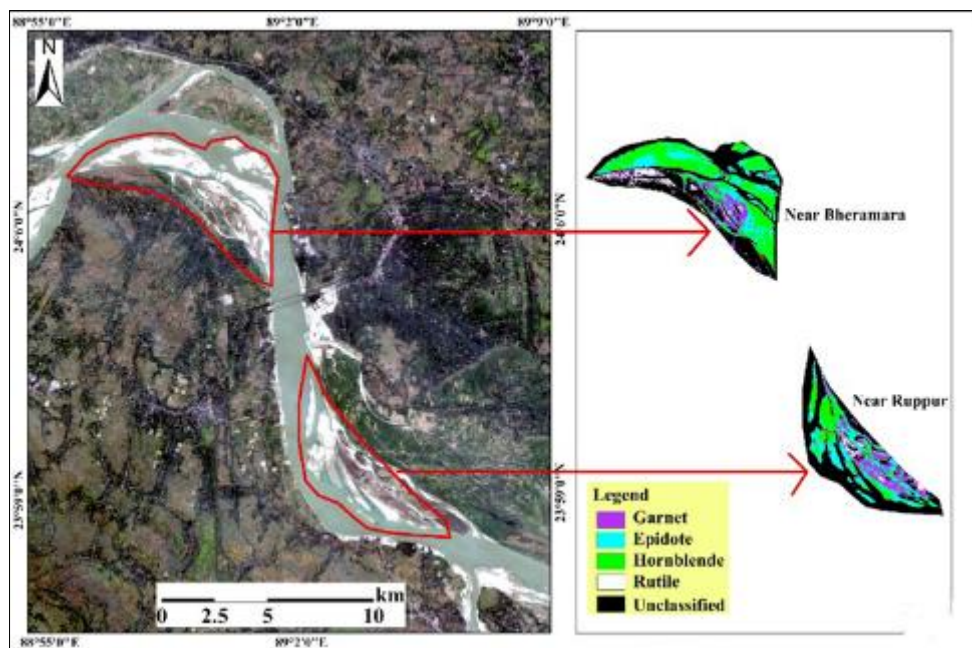

Figure 15 Heavy mineral concentrations from the locations of collected samples

4.2. Mineralogical concentration from microscopic grain counting

Individual heavy mineral concentration is calculated by the microscopic grain counting method. More than 15 types of minerals are being identified under the microscope in the study area. These include the economically important heavy minerals biotite, epidote, garnet, hornblende, kyanite, monazite, rutile, hematite, ilmenite and magnetite, which are the most common in the area (Table 3). Moreover, light minerals quartz, feldspar with some lithic fragments are also common in the study area among which quartz is the most abundant light mineral (Table 4).

Table 3 Weight percentages of heavy minerals in the study area from microscopic observation

Sample ID	Biotite	Epidote	Garnet	Hornblende	Kyanite	Monazite	Rutile	Hematite	Ilmenite	Magnetite
BM-1	5.15	13.08	14.62	8.95	14.85	4.99	10.05	6.38	5.92	16.01
BM-2	4.93	13.59	13.44	9.06	15.21	5.07	9.79	6.94	6.56	15.41
BM-3	4.85	12.88	14.06	9.18	14.94	5.12	9.93	7.90	5.10	16.04
BM-4	4.84	13.10	13.90	8.85	14.86	5.69	10.04	6.89	6.01	15.84
BM-5	4.86	13.20	13.88	8.91	14.88	5.82	9.97	6.73	6.56	15.19
RP-1	4.95	13.18	13.95	8.97	14.93	6.01	9.94	6.96	7.03	14.08
RP-2	4.99	13.15	13.89	9.02	15.11	5.98	9.99	7.01	6.85	14.01
RP-3	4.92	13.12	14.03	9.05	15.08	5.99	10.02	7.07	6.79	13.93
RP-4	4.85	13.20	13.98	8.99	14.96	6.03	10.05	7.02	6.89	14.03
RP-5	5.02	13.07	14.17	8.92	14.88	5.87	9.98	6.92	6.77	14.40
Average	4.93	13.16	13.99	8.99	14.97	5.65	9.98	6.98	6.44	14.89

Table 4 Weight percentages of light minerals in the study area from microscopic observation

Sample ID	Quartz	Feldspar	Lithic Fragments
BM-1	51.22	39.02	9.76
BM-2	57.23	34.43	8.34
BM-3	56.41	35.89	7.69
BM-4	59.63	32.45	7.92
BM-5	65.79	28.94	5.26
RP-1	59.46	32.43	8.11
RP-2	57.98	34.60	7.42
RP-3	58.97	33.33	7.69
RP-4	62.55	28.78	8.67
RP-5	68.75	25.71	5.71

4.3. Mode of sediment transportation

The histograms (Figure 9) and frequency curves (Figure 10) obtained from sieve analysis of the sediment samples indicates that the mode transportation is unimodal. Cumulative frequency curve helps to determine the population of the sediments generally occurred in three segments namely traction, saltation and suspension population. Six cumulative curves (Figure 11) from the collected samples show that the transportation mode of all samples is mostly saltation population (Table 5), which reflects a form of transport for sediment by rivers in the study area.

Table 5 Mode of sediment transportation percentages of the samples in the study area

Sample ID	Traction	Saltation	Suspension
BM-1	0.55	87.23	12.22
BM-3	0.37	88.73	10.90
BM-5	0.52	89.74	9.74
RP-1	0.96	89.05	9.99
RP-3	1.84	82.67	15.49
RP-5	3.86	68.70	27.44

4.4. Socio-economic importance of the minerals

Garnet, epidote, hornblende, kyanite, rutile, and quartz are minerals with significant socio-economic implications, especially when identified using remote sensing technologies. Remote sensing allows for large-scale, cost-effective exploration and monitoring of these minerals, which is important for efficient resource management and development. Garnet, with its uses in abrasives, gemstones, and as a filter material, plays a vital role in the industrial sector. Epidote is important in mining and construction due to its association with ore deposits and its influence on rock stability. Hornblende, a common amphibole mineral, is used in the construction industry and as a geological indicator for evaluating mineral deposits. Kyanite is valued in the production of high-temperature ceramics and refractory materials, essential for manufacturing and industry. Rutile, a primary source of titanium, is crucial for aerospace, defense, and various high-tech industries due to its strength and corrosion resistance. Quartz, being one of the most versatile minerals, has applications ranging from electronics to glassmaking. Remote sensing facilitates the efficient discovery and management of these minerals by providing accurate, comprehensive data in mineral distribution and concentration, thus supporting sustainable resource utilization and economic development. Sustainable development necessitates an appropriate balance between social, economic, and environmental well-being, both in the present and for future generations (Marker et al., 2005) [33]. Energy and mineral resources constitute the primary sources of socio-economic growth for a nation, as numerous production and consumption activities involve energy as a fundamental input (Ali et al., 2022) [34]. The mineral resources thus far discovered in Bangladesh are limited in comparison to its substantial population. To meet the demand of this fast growing population and achieve sustainable development, additional mineral resources must be discovered and developed (Akhtar, 2005) [35]. In developing nations, the mineral industry plays a crucial role (ESCAP, 1999) [36]. A country's standard of living is partially determined by how effectively it utilizes its undiscovered mineral resources and develops industries based on these minerals [35]. For the successful exploration and exploitation of hidden mineral resources, a critical factor is a robust economic foundation, which represents a significant challenge for developing nations like Bangladesh [35].

5. Conclusion

The study area is rich in biotite, epidote, garnet, hornblende, kyanite, monazite, rutile, hematite, ilmenite and magnetite from sediment samples among which garnet (13.99%), epidote (13.16%), hornblende (8.99%), kyanite (14.97%) and rutile (9.98%) are the most abundant with socio-economic importance. Though quartz is not a heavy mineral, its abundance in the study area is economically valuable. Most of these economically important heavy minerals are identified and their concentrations are mapped from multispectral Landsat-9 (OLI/TIRS) satellite image using ENVI 5.3 software. The purpose of sustainable exploitation techniques for the heavy mineral resources in this area can be easily fulfilled by this image analysis process without hampering the localities. The valuable heavy minerals found in the Padma river bar sediments from Bheramara to Ruppur can be very resourceful for the country.

Compliance with ethical standards

Disclosure of conflict of interest

The authors unanimously declare there are no conflict of interest in this research work.

References

[1] Rahman MA, Pownceby MI, Haque N, Bruckard WJ, Zaman MN. Characterisation of titanium-rich heavy mineral concentrates from the Brahmaputra River basin, Bangladesh. Applied Earth Science. 2014 Dec;123(4):222-33.

[2] Rahman MA, Pownceby MI, Haque N, Bruckard WJ, Zaman MN. Valuable heavy minerals from the Brahmaputra River sands of Northern Bangladesh. Applied Earth Science. 2016 Sep;125(3):174-88.

[3] Rahman MJ, Pownceby MI, Rana MS. Occurrence and distribution of valuable heavy minerals in sand deposits of the Jamuna River, Bangladesh. Ore Geology Reviews. 2020 Jan 1; 116:103273.

[4] Chandrasekar N, Mujabar PS, Rajamanickam GV. Investigation of heavy-mineral deposits using multispectral satellite data. International journal of remote sensing. 2011 Dec 10;32(23):8641-55.

[5] Ahmadirouhani R, Karimpour MH, Rahimi B, Malekzadeh-Shafaroudi A, Pour AB, Pradhan B. Integration of SPOT-5 and ASTER satellite data for structural tracing and hydrothermal alteration mineral mapping: Implications for Cu–Au prospecting. International Journal of Image and Data Fusion. 2018 Jul 3;9(3):237-62.

[6] Rajendran S, Nasir S. ASTER capability in mapping of mineral resources of arid region: A review on mapping of mineral resources of the Sultanate of Oman. Ore Geology Reviews. 2019 May 1; 108:33-53.

[7] Bolouki SM, Ramazi HR, Maghsoudi A, Beiranvand Pour A, Sohrabi G. A remote sensing-based application of Bayesian networks for epithermal gold potential mapping in Ahar-Arasbaran Area, NW Iran. Remote Sensing. 2019 Dec 27;12(1):105.

[8] Reeves RG. Manual of remote sensing, 1, 2 (Falls Church VA: American Society of Photogrammetry); 1975.

[9] Siegal BS, Gillespie AR, Siegal BS, editors. Remote sensing in geology. New York: Wiley; 1980 Sep 25.

[10] Carper W, Lillesand T, Kiefer R. The use of intensity-hue-saturation transformations for merging SPOT panchromatic and multispectral image data. Photogrammetric Engineering and remote sensing. 1990 Apr 1;56(4):459-67.

[11] Gabr S, Ghulam A, Kusky T. Detecting areas of high-potential gold mineralization using ASTER data. Ore Geology Reviews. 2010 Oct 1;38(1-2):59-69.

[12] Bedini E. Mineral mapping in the Kap Simpson complex, central East Greenland, using HyMap and ASTER remote sensing data. Advances in Space Research. 2011 Jan 4;47(1):60-73.

[13] Tangestani MH, Jaffari L, Vincent RK, Sridhar BM. Spectral characterization and ASTER-based lithological mapping of an ophiolite complex: A case study from Neyriz ophiolite, SW Iran. Remote Sensing of Environment. 2011 Sep 15;115(9):2243-54.

[14] Van der Meer FD, Van der Werff HM, Van Ruitenbeek FJ, Hecker CA, Bakker WH, Noomen MF, Van Der Meijde M, Carranza EJ, De Smeth JB, Woldai T. Multi-and hyperspectral geologic remote sensing: A review. International journal of applied Earth observation and geoinformation. 2012 Feb 1;14(1):112-28.

[15] Zoheir B, Emam A. Field and ASTER imagery data for the setting of gold mineralization in Western Allaqi–Heiani belt, Egypt: A case study from the Haimur deposit. Journal of African Earth Sciences. 2014 Nov 1; 99:150-64.

[16] Qari MH, Madani AA, Matsah MI, Hamimi Z. Utilization of Aster and Landsat data in geologic mapping of basement rocks of Arafat Area, Saudi Arabia. The Arabian Journal for Science and Engineering. 2008 Jun 1;33(1C):99-116.

[17] Sadeghi M, Jones SB, Philpot WD. A linear physically-based model for remote sensing of soil moisture using short wave infrared bands. Remote Sensing of Environment. 2015 Jul 1; 164:66-76.

[18] Pournamdari M, Hashim M, Pour AB. Application of ASTER and Landsat TM Data for Geological Mapping of Esfandagheh Ophiolite Complex, Southern I ran. Resource Geology. 2014 Jul;64(3):233-46.

[19] Adiri Z, Harti AE, Jellouli A, Maacha L, Bachaoui EM. Lithological mapping using Landsat 8 OLI and Terra ASTER multispectral data in the Bas Drâa inlier, Moroccan Anti Atlas. Journal of Applied Remote Sensing. 2016 Jan 1;10(1):016005-.

[20] Ourhzif Z, Algouti A, Hadach F. Lithological mapping using landsat 8 oli and aster multispectral data in imini-ounilla district south high atlas of marrakech. The International Archives of the Photogrammetry, Remote Sensing and Spatial Information Sciences. 2019 Jun 5; 42:1255-62.

[21] Kruse FA, Bedell RL, Taranik JV, Peppin WA, Weatherbee O, Calvin WM. Mapping alteration minerals at prospect, outcrop and drill core scales using imaging spectrometry. International Journal of Remote Sensing. 2012 Mar 20;33(6):1780-98.

[22] Guha DK. Tectonic framework and oil and gas prospects of Bangladesh. InProc. 4th Annual Conference, Bangladesh Geological Society, Dhaka 1978 (pp. 65-76).

[23] Reimann KU, Hiller K. Geology of Bangladesh; 1993.

[24] Geological Survey of Bangladesh, Alam MK, Hasan AS, Khan MR, Whitney JW, Abdullah SK, Queen JE. Geological map of Bangladesh. Geological Survey of Bangladesh; 1990.

[25] Kruse FA, Boardman JW, Huntington JF. Comparison of airborne hyperspectral data and EO-1 Hyperion for mineral mapping. IEEE transactions on Geoscience and Remote Sensing. 2003 Jun;41(6):1388-400.

[26] Joseph W. Automated spectral analysis: A geologic example using AVIRIS data, north Grapevine Mountains, Nevada. InProc. Tenth Thematic Conference on Geologic Remote Sensing, Environmental Research Institute of Michigan 1994 (pp. 1407-1418).

[27] Boardman JW. Automating spectral unmixing of AVIRIS data using convex geometry concepts. InJPL, Summaries of the 4th Annual JPL Airborne Geoscience Workshop. Volume 1: AVIRIS Workshop 1993 Oct 25.

[28] Boardman JW, Kruse FA, Green RO. Mapping target signatures via partial unmixing of AVIRIS data. In Summaries of the fifth annual JPL airborne earth science workshop. Volume 1: AVIRIS workshop 1995 Jan 23.

[29] Yuhas RH, Goetz AF, Boardman JW. Discrimination among semi-arid landscape endmembers using the spectral angle mapper (SAM) algorithm. InJPL, Summaries of the Third Annual JPL Airborne Geoscience Workshop. Volume 1: AVIRIS Workshop 1992 Jun 1.

[30] Van der Meer FD, de Jong SJ. Spectral mapping methods: many problems, some solutions. InProceedings of the 3rd EARSeL workshop on imaging spectroscopy, Herrsching, Germany, 13-16 May 2003/ed. by M. Habermeyer, A. Mülle and S. Holzwarth. EARSeL. pp. 146-162 2003 (pp. 146-162). EARSeL.

[31] Boggs Jr S. Petrology of sedimentary rocks. Cambridge university press; 2009 Feb 19.

[32] Friedman GM, Sanders JE. Principles of sedimentology; 1978.

[33] Marker, Brian R., et al. "Sustainable minerals operations in the developing world: introduction." Geological Society, London, Special Publications 250.1 (2005): 1-4.

[34] Ali, Minhaj, et al. "The nexus between remittances, natural resources, technological innovation, economic growth, and environmental sustainability in Pakistan." Environmental Science and Pollution Research 29.50 (2022): 75822-75840.

[35] Akhtar, Afia. "Mineral resources and their economic significance in national development: Bangladesh perspective." Geological Society, London, Special Publications 250.1 (2005): 127-134.

[36] ESCAP, UN. "Sustainable development of land and mineral resources in Asia and the Pacific: national policy initiatives and trends in mining taxation." (1999).